ELSEVIER

Journal of Chromatography A, 837 (1999) 139–151

JOURNAL OF CHROMATOGRAPHY A

Flow field-flow fractionation of high-molecular-mass polyacrylamide

R. Hecker[a], P.D. Fawell[b,*], A. Jefferson[a], J.B. Farrow[b]

[a] *A.J. Parker Cooperative Research Center for Hydrometallurgy, School of Applied Chemistry, Curtin University of Technology, GPO Box U1987, Perth, WA 6845, Australia*

[b] *A.J. Parker Cooperative Research Center for Hydrometallurgy, CSIRO Minerals, P.O. Box 90, Bentley, WA 6102, Australia*

Received 7 July 1998; received in revised form 11 December 1998; accepted 23 December 1998

Abstract

The fractionation of high-molecular-mass polyacrylamide in aqueous solutions by size-exclusion chromatography is complicated by concerns over adsorption and shear degradation. The coupling of flow field-flow fractionation (flow FFF), multi-angle laser light scattering (MALLS) detection and a concentration-sensitive detector provided absolute measurement of molecular mass distributions in a low shear environment. Critical to the success of the method was the careful selection of the carrier solution. A number of commercial polyacrylamide standards with mean molecular masses in the range 0.35 to $9.00 \cdot 10^6$ were studied. The breadth of the distributions indicated the presence of entangled or agglomerated polymer. Diffusion coefficients calculated from both light scattering and flow FFF retention were comparable, as well as being consistent with extrapolations from literature values for lower-molecular-mass polyacrylamides.

Keywords: Flow field-flow fractionation; Field-flow fractionation; Multi-angle laser light scattering; Diffusion; Molecular mass distribution; Agglomerates; Polyacrylamide

1. Introduction

The application of polymers to the flocculation of both mineral and organic substrates utilises primarily high-molecular-mass polyacrylamide (PAAm) and derivatives with a weight-average molecular mass M_w in the range $10–20 \cdot 10^6$ [1,2]. The most widely accepted model of flocculation requires that a single polymer coil is adsorbed to two or more particulate surfaces simultaneously to bridge and create a rapidly settling aggregate. The effect of mixing, shear and particulate surface chemistry on flocculation has been extensively studied [3–5] but the effect of polymer mass distribution is essentially unknown. Feasibly the smaller molecular mass fraction diffuses onto the surface more rapidly but the larger mass fractions are more able to bind onto surfaces and across particles [6,7]. An accurate study of flocculation requires knowledge of the molecular mass distribution of the flocculant.

Size-exclusion chromatography (SEC) is the most common tool for characterisation of polymer mass distributions, but separation by the exclusion effect occurs in a gel-packed column. The viscosity and shear-sensitivity of high-molecular-mass PAAm is incompatible with high flow-rates through a packed column, and consequently experiments may take tens of hours to avoid polymer degradation [8].

The field-flow fractionation (FFF) family of tech-

*Corresponding author. Fax: +61-8-9334-8001.
E-mail address: Phillip.Fawell@minerals.csiro.au (P.D. Fawell)

0021-9673/99/$ – see front matter
PII: S0021-9673(99)00070-9

niques feature an open channel and little exposed surface (approximately 0.01 m^2) such that analytical error from adsorptive loss and shearing are limited [9]. FFF relies on the competition on the analyte between the drift force of the field and, for samples less than 1 μm diameter, the entropically driven back diffusion off the accumulation wall. The narrow ribbon-shaped channel is sufficiently thin such that the carrier flow profile is parabolic, and the mean position of smaller, more diffusive samples occupy a range of faster-moving laminae, as shown in Fig. 1.

The subtechniques of FFF arise from the nature of applied field. For the analysis of synthetic polymers both thermal gradient (thermal FFF) and crossflow (flow FFF) fields have been shown to be effective [10–12]. The universal nature of flow FFF, in that all samples are influenced by crossflow, is advantageous but the presence of a membrane within the channel often leads to excess band broadening due to surface roughness and interactions between the solute and the membrane. A comparison of the elution of polyvinylpyridine [13] shows broader peaks and slower elution of samples from flow FFF as compared to the mirror-smooth thermal FFF cell, although for aqueous media the latter was ineffective due to poor thermal diffusion in water [14–16].

The use of multi-angle laser light scattering (MALLS) to determine macromolecular parameters of root-mean-square radii and molecular mass has been described elsewhere [17]. Installing such a detector to a flow arrangement and introducing a concentration-sensitive device allows light scattering to be used for chromatographic detection [18]. This FFF–MALLS combination has been applied to fractionating model systems of polystyrene latices [19–21] and sulphonated polystyrenes [22].

Fractionation of PAAm by flow FFF has been reported for standards with nominal molecular masses of up to $1.4 \cdot 10^6$ [13]. No publication yet reports fractionation of higher molecular mass PAAm, nor the application of the FFF–MALLS combination to PAAm analysis. This work sets out the method development for the fractionation of PAAm by FFF–MALLS and comparison of molecular masses determined by light scattering with the molecular masses from diffusion coefficients.

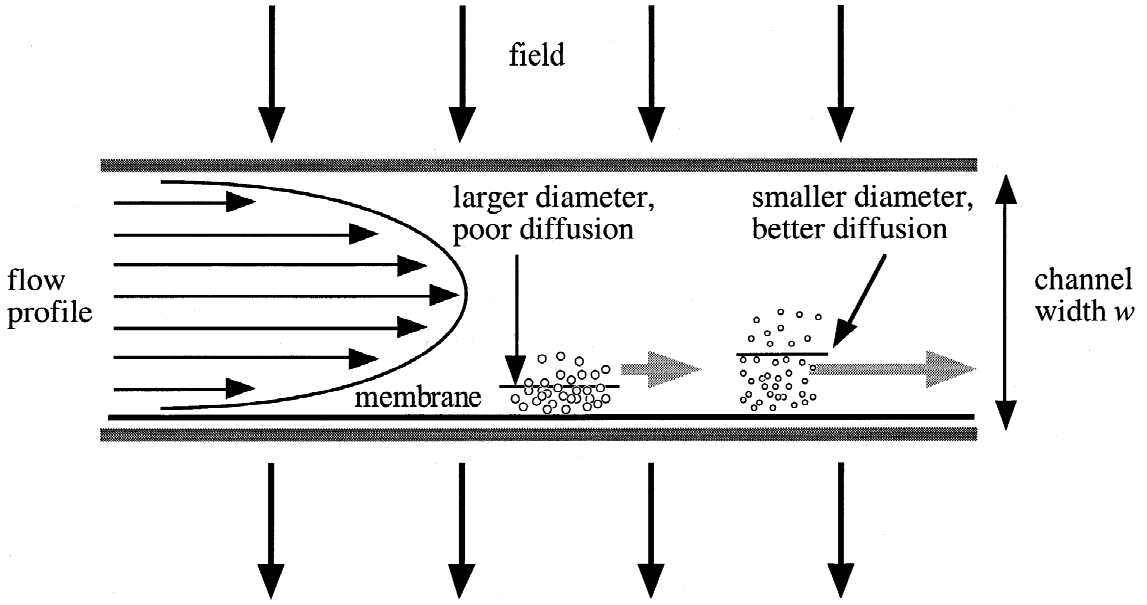

Fig. 1. Mechanism of FFF for submicron-sized solutes: smaller samples diffuse effectively against the field so the mean position of the sample is further from the membrane.

2. Theory

2.1. Flow field-flow fractionation

FFF possesses, unlike most chromatographic techniques, a reliable theoretical basis for prediction of elution times [23–25]. Under model conditions, flow FFF retention times for submicron diameter particles depend solely upon diffusion coefficient D (the ''normal mode'' operation) by

$$D = \frac{w^2}{6t_r}\left(\frac{\dot{V}_c}{\dot{V}}\right) \quad (1)$$

where t_r is the retention time of the species with diffusion coefficient D in a channel of thickness w and flow-rates $\dot{V}_c$ and $\dot{V}$ for cross- (field) and channel-flow, respectively. Since, from the Stokes–Einstein equation

$$d_s = \frac{kT}{3\pi\eta D} \quad (2)$$

the diffusion coefficient is inversely proportional to the Stokes' diameter of the sample (d_s), analyte size can be calculated from flow FFF retention time. For polydisperse samples the problem of producing separation within a reasonable experimental time arises. For FFF this may be solved by allowing the field strength to decay over the course of the separation. For an exponential decay, where the field decreases from an initial crossflow $\dot{V}_c^i$ with a time constant τ, the field strength after time t is given by

$$\dot{V}_c(t) = \dot{V}_c^i \exp\left(-\frac{t}{\tau}\right) \quad (3)$$

which upon integrating and substitution into Eq. (1) gives

$$D = \frac{w^2}{6}\frac{\dot{V}_c^i}{\dot{V}}\left[\tau\left(\exp\left(\frac{t_r}{\tau}\right) - 1\right)\right]^{-1} \quad (4)$$

This result shows that the measured diffusion coefficient is a straightforward function of retention time.

2.2. Light scattering

Theory for the MALLS laser photometer is provided by Wyatt [17]. Measurement of the scattered light at a number of angles gives the absolute mean molecular mass, provided corrections for refraction effects and detector response are included. When coupled to a fractionator, an on-line concentration detector (i.e., refractive index or spectrophotometric) is required, which for a given effluent slice the following equation (shown here to second order) exhibits the relation of scattering to molecular mass

$$\frac{R_\theta}{K^* c} = M_w P(\theta) - 2A_2 M_w^2 P^2(\theta)c + \cdots \quad (5)$$

where R_θ is the scattering intensity excess to solvent scattering for solute of concentration c and weight average molecular mass M_w. The K^* term is a scattering constant dependent upon the wavelength of incident light λ_0, the refractive index of the solvent and the square of the refractive index increment with concentration, $\frac{dn}{dc}$. The function $P(\theta)$ is an architecture function for random coil geometry dependent upon the proximity of scattering centres throughout the molecule

$$P(\theta) = 1 - \frac{2\mu^2\langle r^2\rangle}{3!} + \cdots \quad (6)$$

where $\mu = \left(\frac{4\pi}{\lambda_0}\right)\sin\left(\frac{\theta}{2}\right)$. The value of $\langle r^2\rangle^{0.5}$ is known as the root-mean-square radius (''rms radius''), derived from the distribution of the scattering centres with respect to a central position. The equation holds only if $\mu^2\langle r^2\rangle << 1$, a condition that requires that two waves of light encountering the same molecule must not be overly out of phase.

From these light scattering equations, it can been seen that plotting $\frac{R_\theta}{K^* c}$ from the detector set versus $\sin^2\left(\frac{\theta}{2}\right)$ gives, upon extrapolation to $\theta = 0°$, the value for M_w provided the concentration for the effluent slice is known accurately from the on-line refractometer. Sources of error arising include accurate determination of the solvent refractive index, refractive index increment and solute concentration.

2.3. Molecular mass calculation

With a MALLS detector characterising FFF effluent, molecular mass can be calculated in two

ways. Direct measurements arise when the FFF acts passively separating the sample into near monodisperse slices for treatment by the MALLS according to the requirements of Eq. (5). Molecular masses may also be calculated indirectly from FFF retention. Eq. (4) shows retention is dependent solely upon the diffusion coefficient for flow FFF under normal mode operations. The diffusion coefficient is in turn strongly dependent upon molecular mass according to the standard expression

$$D = AM_w^b \quad (7)$$

where A and b are empirically-determined constants for a given polymer–solvent–temperature system. Substitution of Eq. (7) into Eq. (4) gives the final indirect determination of molecular mass.

3. Experimental

3.1. Reagents

Purified water was obtained from a Milli-Q Plus 185 unit with resistivity >18 MΩ/cm (Millipore, Bedford, MA, USA). Analytical-reagent grade formamide, nitric and acetic acid (BDH, Poole, UK) were used as received. All dilute solutions were freshly vacuum filtered through a 0.22 μm filter (Millipore, type GV).

Polyacrylamide standards were obtained from Polymer Labs. (Birmingham, UK) with cited weight-averaged molecular masses 0.35, 1.14, 5.55 and $9.00 \cdot 10^6$ and polydispersity index ca. 2.3. A commercial nonionic polyacrylamide flocculant with a weight-averaged molecular mass of approximately $2 \cdot 10^7$ was used for the shear study. Aqueous solutions were prepared in Milli-Q water freshly filtered through a 0.02-μm syringe filter (Anotop 25 Plus, Whatman, Maidstone, UK). PAAm stock solutions were produced by adding portions of polymer piecewise to solvent pretared in a screwtop glass jar, then shaken overnight on an orbital shaker at 150 ± 5 rpm (Braun TM-1, Basel, Switzerland). All solutions were prepared in a laminar flow cabinet (Gelman HWS, Ann Arbor, MI, USA).

Polystyrene–divinylbenzene latex standards were purchased from Duke Scientific (Palo Alto, CA, USA). The latex sample diameters were characterised by the manufacturer using electron microscopy.

3.2. Apparatus

The flow FFF cell was a model F0-1000 from FFFractionation (Salt Lake City, UT, USA) featuring ceramic depletion and accumulation walls. The accumulation wall was covered by a membrane of regenerated cellulose (nominal molecular mass cut-off 10^4) from FFFractionation. The channel shape was defined by a PTFE spacer 0.25 mm thick, 300 mm long and 20 mm maximum width. The final 20 mm of the channel immediately prior to the sample outlet was fitted with a frit outlet device.

Both channel and crossflow were delivered by dual-piston pumps (LC10-AD, Shimadzu, Kyoto, Japan) followed by a 680 kPa backpressure regulator allowing the pump checkvalves to operate properly. The crossflow was continually recycled. The channel flow was fed to the pump from the reservoir through a 10-μm sink filter, an in-line degasser unit (Shimadzu GT-102), while after the pump the carrier passed through a 0.1-μm filter (Millipore type VV).

All flows were carried by 0.51 mm I.D. polyether ether ketone (PEEK) tubing. Channel flow was diverted through a 10-port two-position valve (Valco, Houston, TX, USA), through a sample injector (Rheodyne 7125, Cotati, CA, USA) and into the FFF cell. The sample outlet passed through the detectors, returned through the valve, a 275 kPa backpressure regulator and to waste. The frit outlet line passed to the Valco valve, then to a needle valve (Nupro, Willoughby, OH, USA) controlling the flow splitting between the detector and frit outlet lines, then to waste.

Injections into the FFF apparatus were made with a 250 μl syringe, loaded to at least 50% over the sample loop volume. For polyacrylamides the shear sensitivity required slow loading, with a typical 150 μl load taking 1.5 min, as more rapid loading produced artefacts in the fractograms. In all cases the syringe was rinsed with five loadings of carrier liquid, as was the injector. Without these protocols cross-contamination occurred.

Detectors for the FFF effluent were spectrophotometric (SPD-10AV, Shimadzu), laser light scattering (Dawn-DSP from Wyatt Technology, Santa Barbara,

CA, USA) and a differential refractometer (DRI, Optilab 903, Wyatt Technology). The spectrophotometric detector featured an 8-μl cell and observed at 230 nm. The light scattering detector used a 632 nm vertically polarised He–Ne laser with the 15 detectors calibrated with triply 0.02 μm filtered toluene and normalised with a 0.2 μm filtered dextran T-10 (Pharmacia, Uppsala, Sweden) solvated by the FFF carrier solution. The refractometer used a 632 nm source and a 10-mm P100 cell, maintained at 35.0±0.1°C by a waterbath (Grant, Cambridge, UK) and calibrated with a series of sodium chloride solutions. The DRI was reset before each fractionation experiment. After each fractionation the apparatus was left to run freely for at least an hour. Data accumulation for the detectors used Wyatt Technology ASTRA 4.1 software.

For all FFF experiments a pre-experiment time was used to give a baseline for detectors, a sample load time chosen sufficient for the channel flow to sweep out 1.2 volumes from injector to fractionator, and a stopflow relaxation time was chosen such that the field flow clears one channel void volume. Standard PAAm analysis flows were channel flow 0.3 ml/min and initial field flow of 0.4 ml/min, while a 5.5 min baseline accumulation time until injection, 0.5 min load time and 4.0 min stopflow time occurred before fractionation commenced.

3.3. Shear studies

Concentrated (5 mg/ml) and dilute (0.5 mg/ml) aqueous solutions of $2 \cdot 10^7$ molecular mass polyacrylamide were prepared using procedures described above. A solution sample was collected into a syringe and extruded through 0.3 to 2.4 m lengths of PEEK tubing of internal diameter 0.26 and 0.51 mm (0.010 in. and 0.020 in.) at flow-rates from 0.2 to 1.2 ml/min controlled by a Razel syringe pump (Stamford, CT, USA). Effluent from the shearing tube flowed into the Dawn-DSP light scattering cell and out for collection for agglomeration studies.

3.4. Agglomerate size distribution

The size distributions of agglomerates in PAAm solutions were measured with a Hiac/Royco 9064 ''sizing counter'' (Pacific Scientific, Silver Spring, MD, USA) fitted with a MicroCount-05 liquid sensor and controlled by the Hiac/Royco Particle Distribution Analysis Software (PDAS, Version 2.1). Flow past the detectors (60 ml/min) was initiated by applying overpressure to the solution with compressed air equipped with an AW3000 filter-regulator (SMC, Sydney, Australia) adjusted to 75 kPa over atmospheric pressure. The sizing counter provides the number of counts measured over each of a range of size channels. The use of this instrument has been described by Hecker et al. [26].

The polymer solution was collected in a sample vial such that 5.0±0.1 g of polymer solution was added dropwise to 100±0.5 g of water with continual gentle swirling of the vial. Time between the final polymer collection and sampling by the sizing counter was no more than 5 min.

3.5. Light scattering data processing

Molecular mass determinations used the DRI as the primary concentration detector with a refractive index increment $\left(\frac{dn}{dc}\right)$ of 0.190 ml/g. The UV output was monitored routinely but not used for data processing. A set of MALLS detectors were chosen which produce the lowest residual error of molecular mass. This detector set was used consistently. For the chromatographic output fitting by the Debye formalism with a fourth-order angular dependence gave the most reasonable results with the lowest error for all experiments.

3.6. Static ultraviolet spectra

The UV spectra of selected solutions was measured on a Hewlett-Packard 8452A diode array spectrophotometer (Palo Alto, CA, USA) using quartz cells of path length 10 mm.

4. Results and discussion

4.1. The effect of shear on polyacrylamide in solution

Resolution optimisation for liquid chromatography requires minimising dead and void volumes, as well

as limiting longitudinal diffusion and band broadening through shorter analysis times. Reducing the void volume is typically achieved by using thinner tubing, while short analysis time needs rapid solution flow. The viscosity of polymer solutions at low shear rates approaches a zero-shear viscosity, dependent upon factors including molecular mass and distribution, branching ratio, concentration and temperature [27,28]. Beyond a critical shear the viscosity increases as the polymer coils unravel to an extended conformation. Depending upon molecular mass, concentration and flow, a network structure may form [28,29], which for PAAm arises from intermolecular hydrogen bonding and coil entanglement. Hence there is a mechanism in which applied shear may result in polymer agglomeration. At higher shear rates the polymer coil becomes fully extended, and chain scission is likely, irreversibly changing the molecular mass distribution.

Prior to attempting to fractionate PAAm, it was necessary to demonstrate that the flow-rates through narrow connecting tubing would not irreversibly alter the polymer through agglomeration of free coils or shear degradation. MALLS is a reliable method for observing coil dimensions in solution, while light obscuration (with the Hiac/Royco sizing counter) has proved sensitive to the presence of polymer agglomerates [26,30]. For this study a high-molecular-mass ($2 \cdot 10^7$) commercial flocculant, previously found to be susceptible to agglomeration [26], was used.

The error in radii determinations by MALLS was at greatest 3%, or approximately 5 nm. Dilute PAAm solutions (0.5 mg/ml) were not significantly affected by shear, with the variations in rms radii for flow-rates 0.2 to 1.2 ml/min remaining well within the error for tubing with internal diameters of 0.26 and 0.51 mm. However, Fig. 2 suggests that a flow-rate effect may exist at a higher PAAm concentration (5 mg/ml). Solutions flowed through longer lengths of 0.51 mm I.D. tubing exhibited an increase in the mean radius under stronger shear.

Solvated PAAm in a dilute unperturbed state takes a Gaussian coil configuration, assuming a loose spherical to random coil shape. However, under shear conditions a polymer coil occupying a range of flow layers may reduce stress by deforming from a sphere to a prolate ellipsoid oriented with the

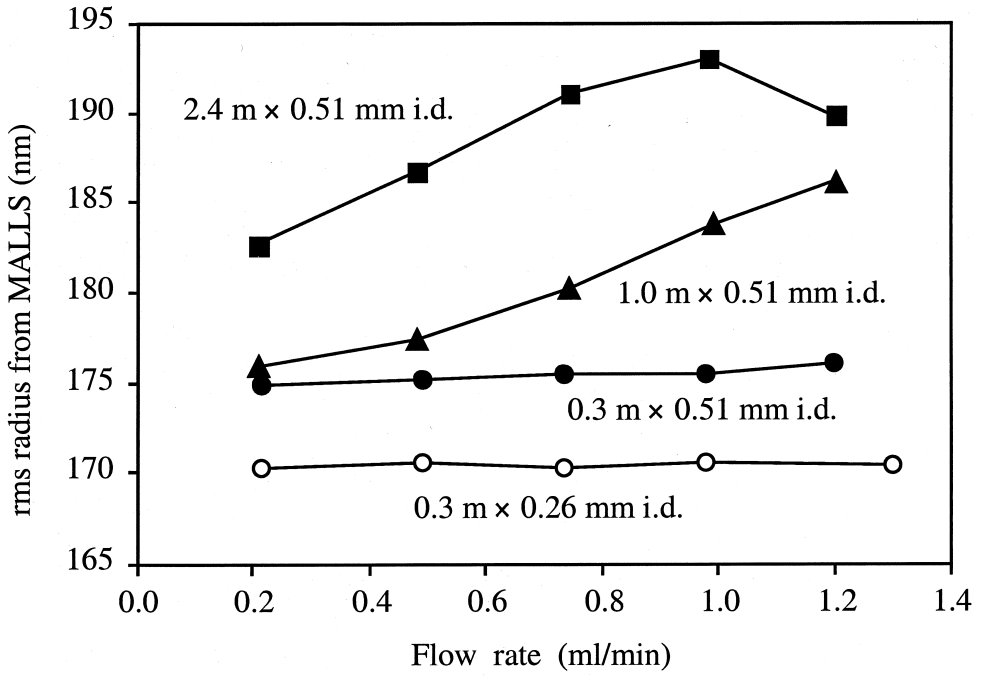

Fig. 2. Effect of tubing dimensions and flow-rate on radius as measured by MALLS for a 5 mg/l solution of PAAm (molecular mass $2 \cdot 10^7$).

direction of flow [31,32]. Beyond a critical strain in this extensional flow polymer solutions experience a coil-stretch transition in which the polymer coil unravels to a highly extended conformation [33]. For a given polymer coil, MALLS will yield a larger rms radius for an ellipsoid than a sphere. The observed increase in rms radius at higher shear for the concentrated PAAm solutions may possibly be attributed solely to this flow deformation.

The effect of shear was investigated further using light obscuration, which provides a count distribution over the size range from 0.7 to 40.0 μm. Fig. 3a shows the counts for each channel for a range of flow-rates through a 0.3 m length of 0.51 mm I.D.

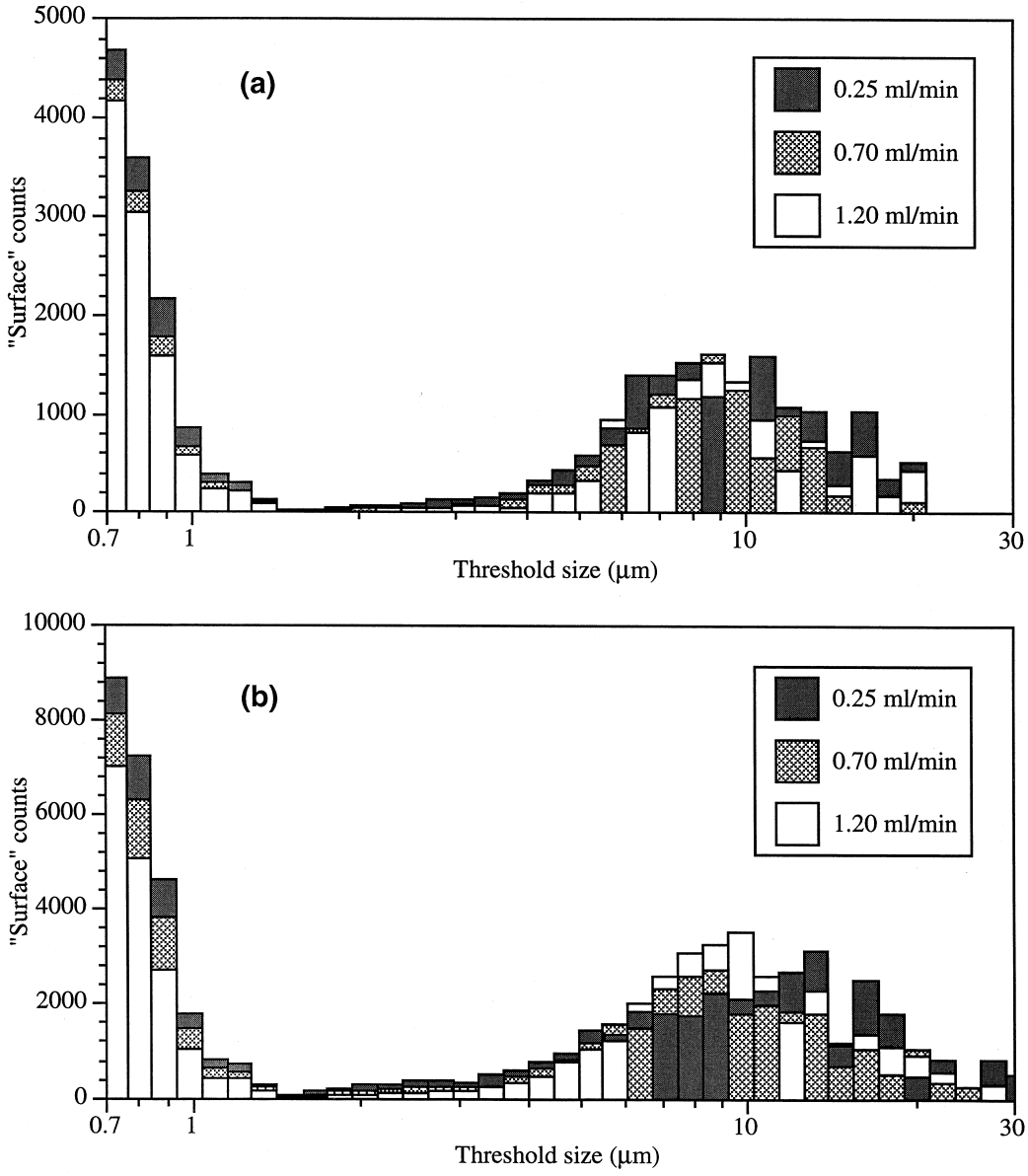

Fig. 3. Agglomerate distribution (presented superimposed) of 5 mg/l PAAm (molecular mass $2 \cdot 10^7$) through 0.51 mm internal diameter tubing of lengths (a) 0.3 m and (b) 2.4 m.

tubing. While no trend with flow-rate was seen, the distributions clearly indicated the presence of agglomerated polymer in the range 5 to 20 μm diameter. Similar behaviour was observed for a 2.4 m length of tubing (Fig. 3b), although the number of counts for each channel almost doubled. The size of these agglomerates is vastly greater than the typical 0.175 μm mean radius observed by MALLS, and suggests they could contain many thousands of polymer chains.

The presence of agglomerates in PAAm solution has been previously noted [26,31,34,35], and may possibly be a consequence of viscosity-shear relationships. The application of shear increases the solution viscosity commensurate with a polymer coil's deformation, but recovery or ''relaxation'' to the initial viscosity is achieved only after some period of no shear. For PAAm, Chmelir et al. [31] observed that this relaxation time ranged from a few minutes to an hour and that the longest times were from the relaxation of a multiple coil agglomerate. Barham [34] found that an individual PAAm coil (molecular mass $3\cdot10^6$) in water took approximately an hour to recover from polymer–polymer entanglement induced by solution flow. The combination of shear stress and residence time (i.e., tube length) allow the polymer time to entangle and form agglomerates.

Unfortunately, the light obscuration technique does not provide full distribution of PAAm sizes from free polymer coils to the largest agglomerates. The technique cannot observe below 0.7 μm, which is much larger than a free coil of ca. 0.35 μm diameter for the flocculant studied. As such the relative fraction of agglomerates in solution cannot be readily assessed. However, the fact that the rms radius as measured by MALLS remains essentially unchanged (other than at the higher polymer concentration and under prolonged shear) indicates that agglomerates over ca. 3.0 μm, while detectable by the sizing counter, are present at a very low concentration. Their number can be also be limited by careful control of the carrier composition [26] and minimising shear in the fractionation system.

4.2. Polyacrylamide fractionation method development

While flow-rates through the fractionator should be kept as low as possible to avoid shear-induced agglomeration, this requirement must be balanced by the need to achieve elution within a reasonable time. By using only 0.51 mm diameter polymer-carrying tubing as short as possible and channel flow-rates of 0.30 ml/min, shear-derived artefacts were avoided as discussed above. Shear is influential for the syringe loading but this was minimised using slow injection.

For a $2.5\cdot10^{-4}$ m wide channel at 298 K and carrier (water) viscosity of $8.904\cdot10^{-4}$ kg/m/s [36] the elution time (t_r, s) for a particle of Stokes diameter d_s under isocratic conditions can be calculated from the following combination of Eqs. (1) and (2)

$$t_r = \frac{\pi\eta w^2}{2kT}\frac{\dot{V}_c}{\dot{V}}d_s \tag{8}$$

This expression is not corrected for the frit outlet, in which the flow through the detectors will be slower, or for local viscosity inhomogenities due to the migrating polymer sample, but it is a good approximation for well-retained samples.

Injection of a 0.265 μm diameter polymer latex gave a peak on elution at 22.4 min under cross- and channel flow-rates of 0.25 and 1.00 ml/min, which upon substitution into the above equation gave a measured Stokes diameter of 0.25 μm. Similarly, injecting a 0.121 μm diameter latex and changing the channel flow to 0.50 ml/min gave a peak after 19.5 min for a calculated diameter of 0.11 μm. The good agreement between the calculated diameter and cited sample value demonstrates satisfactory fractionator operation in this size range.

From the MALLS sizing, PAAm coils of molecular mass $2\cdot10^7$ are approximately 0.35 μm diameter, so for a molecular mass of $1\cdot10^6$ the expected size is 0.09 to 0.15 μm, the range dependent upon polymer configuration. However, injection of aqueous solutions of PAAm standards under the same conditions used for the polymer latex standards consistently resulted in no detectable elution after the void peak. A molecular mass sensitive separation did occur when the stopflow relaxation was not used, albeit with poor resolution. This observation suggested that compressing the polymer even in the gentle crossflow was able to either agglomerate the coils or allow some membrane adsorption effect.

From previous work [26] microgels in PAAm can

be suppressed by the presence of formamide, by favouring polymer–solvent over polymer–polymer interaction. The presence of acetate has a similar effect, and introducing acetate as acetic acid may also protonate the PAAm slightly thereby enhancing intermolecular repulsion. Injections of 20 μl of PAAm standards prepared to 5 mg/ml and aged for two days were made into the FFF cell using a 2% formamide carrier in water adjusted to pH 2.5 with acetic acid. The times to peak maxima are given in Table 1, together with the calculated Stokes diameters.

However, the admixture of formamide and acetic acid adsorb too strongly in the UV range for the weak PAAm chromophores to be detected, and furthermore produce an erratic refractometer baseline. Unusual properties of formamide–acetic acid mixtures have been observed by Verstakov et al. [37]. Acidification of the carrier with a mineral acid (nitric acid) to the same pH eliminated the refractometer oddity. Removing the formamide still allowed successful fractionation of PAAm, demonstrating it is a polymer–membrane interaction suppressed by the acid. The NO_3^- group, like most common anions, also adsorbs below 250 nm [38] obscuring PAAm detection by UV. However, by using more dilute nitric acid, at pH 3.8, a window exists where the polymer is detectable above the nitrate, and the carrier is sufficiently acid to avoid adsorptive loss of the PAAm.

In summary, the optimal carrier for the fractionation of PAAm in a flow FFF cell fitted with a cellulose membrane was found to be dilute nitric acid in Milli-Q water at pH 3.8±0.1, bulk filtered to 0.2 μm.

4.3. Analysis of polyacrylamide standards

A feature of the isocratic experiments described above is excessive band broadening from the slower moving components. Such band broadening may be limited by field programming [12]. Conditions chosen were exponential decay with time constant τ of 60 min with the decay commencing immediately after the end of the stopflow relaxation period. Measured outlet flow-rates remain constant during the fractionation and therefore the interdetector time also remains constant.

A series of PAAm standards prepared in 0.02 μm filtered water at approximately 0.45 mg/ml polymer produced the fractionation profiles shown in Fig. 4, using concentration-sensitive refractive index detection. The stated molecular masses were cited by the manufacturer as a mean molecular mass.

The position of the pre-experiment time and stopflow is clearly seen to the left of the plot. The first sharp peak of the elution profiles may be attributed to the void peak, composed of slight solvent mismatches observed by the refractive index detector, unretained dust and pressure spikes from the stopflow, and as such is of no analytical value.

Fig. 4 also exhibits a degree of overlap in the sample profiles. Caldwell et al. [39] describe the sources of band broadening in terms of injection volume, mass transfer (nonequilibrium) effects and sample polydispersity, but conclude [23] that for polymeric materials the polydispersity contributions are most significant and the fractogram is an accurate representation of the molecular mass distribution.

The presence of artefacts arising from overloading effects manifest as a fronting asymmetry with a shift of peak concentration to shorter retention times [39]. These effects depend strongly upon concentration and viscosity. Fig. 5 shows that for 100 μl injections of a $1.14 \cdot 10^6$ molecular mass PAAm standard at concentrations of 0.43 and 3.75 mg/ml the elution profiles and peak position were unchanged. Loads of up to 375 μg for this standard clearly did not affect the fractionation. The upper limit to the onset of overloading remains unknown, as at higher con-

Table 1
Elution times and calculated sizes of PAAm standards in carrier 2% formamide in water adjusted to pH 2.5 with acetic acid, with channel flow 0.30 and field 0.25 ml/min

M_w of standard	Elution time (peak) (min)	Stokes diameter (calculated) (μm)
$1.14 \cdot 10^6$	18.3	0.062
$5.55 \cdot 10^6$	30.3	0.103
$9.00 \cdot 10^6$	40.0	0.136

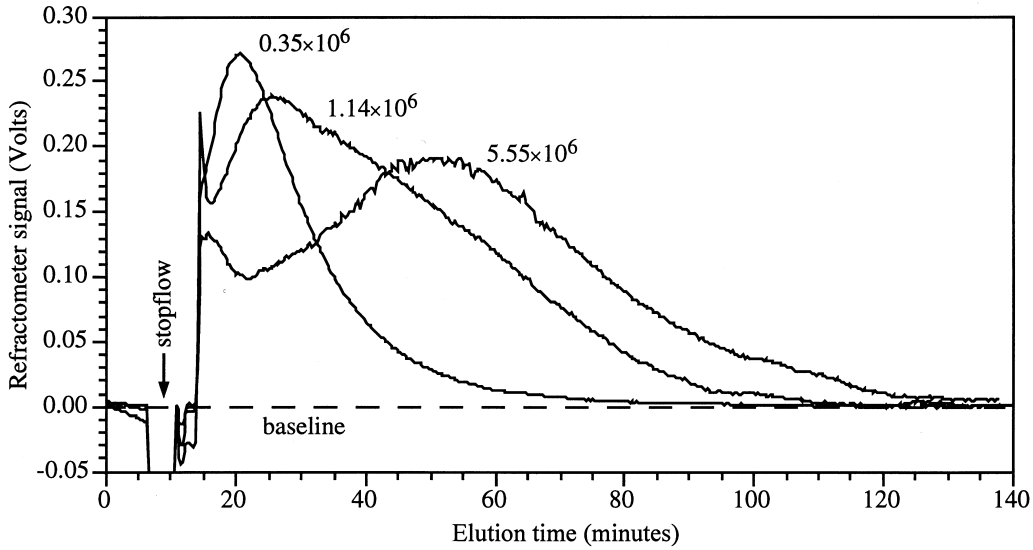

Fig. 4. Flow field-flow fractionation of PAAm standards. Manufacturer-cited molecular masses presented adjacent to the corresponding distribution. Carrier pH 3.8; channel flow 0.30 ml/min and programmed field with initial flow 0.40 ml/min under exponential decay τ 60 min.

centrations injected PAAm becomes unmanageably viscous. The lack of overloading effects is a significant advantage of FFF separations over packed column methods.

Processing the data using the light scattering and including a $9.00 \cdot 10^6$ standard, a molecular mass–elution time relationship is shown in Fig. 6. Good linearity was observed for molecular masses greater than $1 \cdot 10^6$. This demonstrates that a given polymer molecular mass elutes at a reproducible time, in-

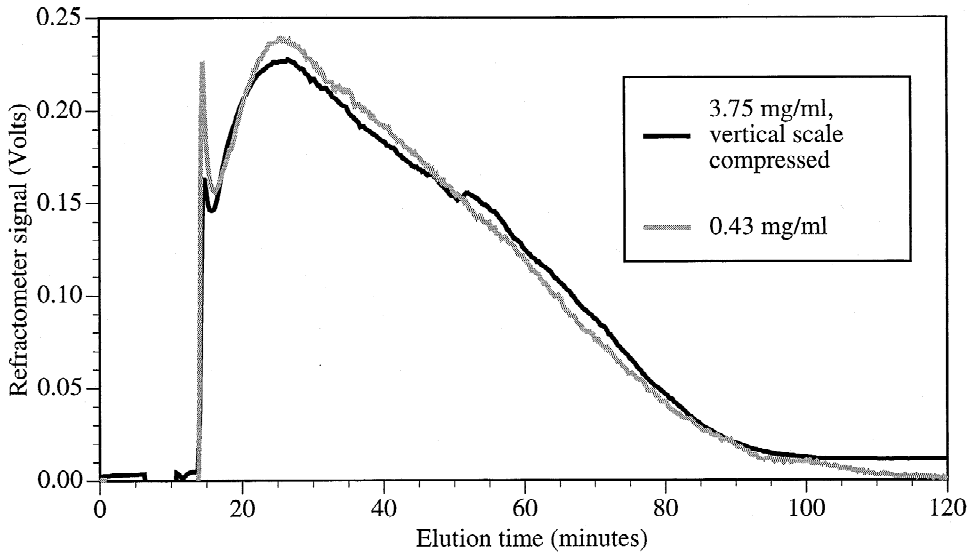

Fig. 5. Concentration effects for $1.14 \cdot 10^6$ standard. Carrier pH 3.8; channel flow 0.30 ml/min and programmed field with initial flow 0.40 ml/min under exponential decay τ 60 min.

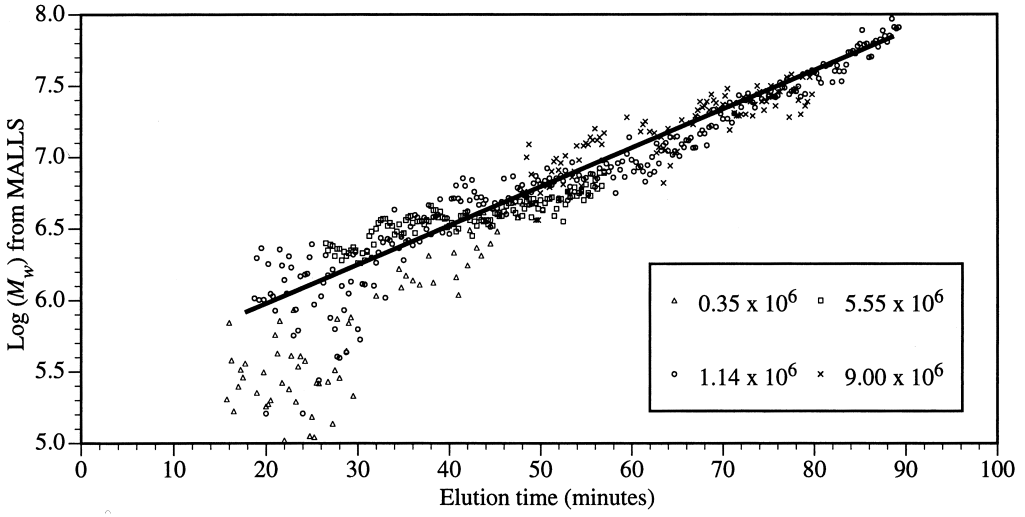

Fig. 6. Molecular mass determinations of PAAm standards. Carrier pH 3.8; channel flow 0.30 ml/min and programmed field with initial flow 0.40 ml/min under exponential decay τ 60 min.

dependent of the source, concluding that the broad fractograms are intrinsic to the standards. Interestingly, the distribution of the $1.14 \cdot 10^6$ molecular mass PAAm standard appears unusually wide, with species of molecular mass up to $50 \cdot 10^6$ present, although it is plausible that they represent many individual polymers intimately coiled. Conformation of this result was achieved by changing the fractionation field decay parameter τ to 90 min. The molecular mass range did not change and the distributions presented in Fig. 6 shifted to a longer time in accordance with Eq. (4).

A significant deviation from linearity was observed for molecular masses below $1 \cdot 10^6$. The primary objective of this study was to develop procedures for the analysis of flocculants, and the fractionation was therefore optimised for molecular masses over $4 \cdot 10^6$. While it would be possible to change the flows to maximise separations at lower molecular masses, band broadening and experimental times for the higher molecular masses would become a concern. The scatter seen in Fig. 6 at short retention times may in part be a consequence of proximity to the void peak.

Recalling the theory section, molecular masses may be evaluated directly via light scattering or indirectly from FFF retention. The light scattering results (direct method) are shown in Fig. 6. The linear regression featured fits well with correlation R^2 of 0.90 and provides an FFF calibration for molecular mass versus elution time. The time axis of Fig. 6 is transformed into a diffusion coefficient for Fig. 7 according to the relationship of Eq. (4). This provides a test of the indirect molecular mass determination.

For comparative purposes two older molecular mass–diffusion coefficient relationships for PAAm are presented, together with the measurement conditions

$$D_A = 8.46 \cdot 10^{-4} M_{SD}^{-0.69}$$

water, 20°C, $0.02 - 0.53 \cdot 10^6$ PAAm (10)

$$D_0 = 1.24 \cdot 10^{-4} M_w^{-0.53 \pm 0.01}$$

0.1 *M* HCl, $0.13 - 8.2 \cdot 10^6$ PAAm (11)

Eq. (10), reported by Scholtan [40], is an area-averaged diffusion coefficient derived from sedimentation measurements of low mass species, while Eq. 11, from Schwartz et al. [41], lacked temperature control, and as such the two are not directly comparable. Extrapolation of the older M_w–D relationships to the higher molecular masses studied here shows the range and domain are consistent, although the gradient is greater than expected. Reasons for this

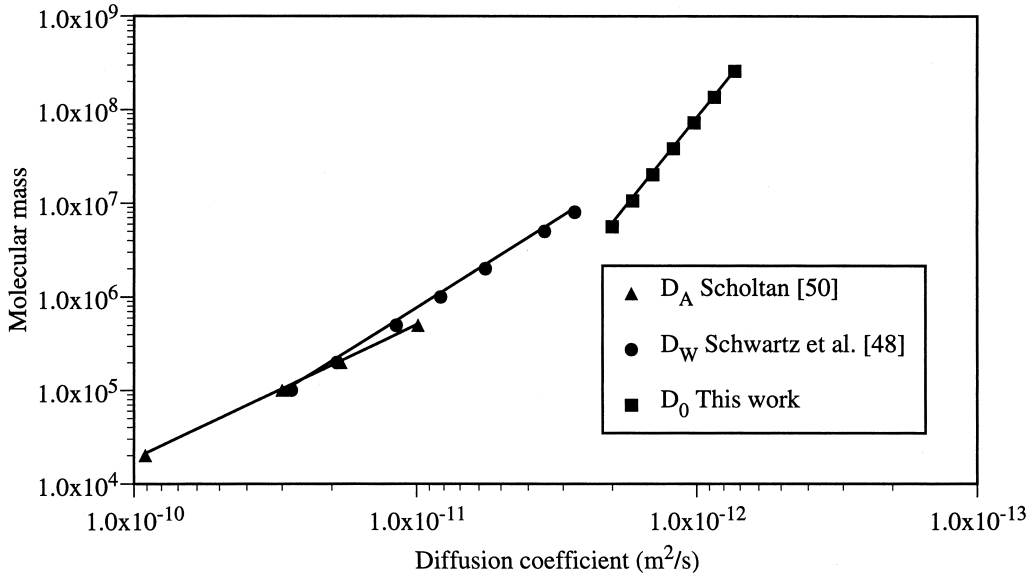

Fig. 7. Empirical diffusion coefficients for PAAm.

include the extreme sensitivity of Fig. 7 to the least-squares fit of Fig. 6, and the presumption that the diffusion coefficients calculated from the FFF are accurate. The last point is significant as it demands immediate sample response to the decaying field, and no analyte–membrane interaction which has been demonstrated from the method development to be an issue. Wyatt [42] has also raised these concerns with regard to FFF theory. Indirect molecular mass measurements, contingent upon ideal fractionator operation and good diffusion–molecular mass conversion may be less reliable than direct light scattering detection for polyacrylamide.

4.4. Comparison with SEC

The upper limit imposed on sample concentration due to viscosity has been a problem in some SEC studies of PAAm, for which the injection of larger sample volumes give the required sensitivity, but at the cost of resolution. For the SEC characterisation of PAAm with a mean M_w of $3 \cdot 10^6$, injected volumes of 0.5 ml were typically required [43], with elution times of over 3 h [8]. The FFF–MALLS technique reported here therefore offers a significant improvement in sensitivity over SEC.

5. Conclusions

Flow field-flow fractionation has been successfully applied to the fractionation of ultra-high-molecular-mass polyacrylamide, with fully elution in less than 2 h. Careful control of the carrier chemistry is required to avoid surface adsorption and loss of sample, while at the same time preventing interference to concentration-sensitive detectors. MALLS detection allow the direct determination of molecular mass distributions for a number of polyacrylamide standards. The relationship between molecular mass and elution time was shown to exhibit a good degree of linearity.

Acknowledgements

This research has been supported under the Australian Government's Cooperative Research Centre (CRC) Program, through the A.J. Parker CRC for Hydrometallurgy. This support is gratefully acknowledged. One of us (R.H.) gratefully acknowledges the support of the ARC by way of an Australian Postgraduate Award through Curtin University of Technology.

References

[1] J. Gregory, C.R. Env. C. 19 (3) (1989) 185.
[2] G.M. Moody, Filtration Sep. 32 (1995) 329.
[3] L.A. Glasgow, Chem. Eng. Prog. 85 (8) (1989) 51.
[4] B.M. Moudgil, S. Behl, T.S. Prakash, J. Colloid Interface Sci. 158 (1993) 511.
[5] R. Hogg, P. Bunnaul, H. Suharyono, Min. Met. Proc. 10 (1993) 81.
[6] G.J. Fleer, Coll. Surf. A 104 (1995) 271.
[7] A.W.M. de Laat, G.L.T. van den Heuvel, Coll. Surf. A 98 (1995) 53.
[8] W.-M. Kulicke, N. Böse, Colloid Polym. Sci. 262 (1984) 197.
[9] J.C. Giddings, Anal. Chem. 67 (1995) 592A.
[10] J.C. Giddings, G.C. Lin, M.N. Myers, J. Liq. Chromatogr. 1 (1978) 1.
[11] Y.S. Gao, K.D. Caldwell, M.N. Myers, J.C. Giddings, Macromolecules 18 (1985) 1272.
[12] K.-G. Wahlund, H.S. Winegarner, K.D. Caldwell, J.C. Giddings, Anal. Chem. 58 (1986) 573.
[13] M.A. Benincasa, J.C. Giddings, J. Microcol. 9 (1997) 479.
[14] J.J. Kirkland, W.W. Yau, J. Chromatogr. 353 (1986) 95.
[15] J.J. Kirkland, C.H. Dilks, S.W. Rementer, Anal. Chem. 64 (1992) 1295.
[16] J.J. Kirkland, C.H. Dilks, Anal. Chem. 64 (1992) 2836.
[17] P.J. Wyatt, Anal. Chim. Acta 272 (1993) 1.
[18] M. Martin, Chromatographia 15 (1982) 426.
[19] D. Roessner, W.-M. Kulicke, J. Chromatogr. A 687 (1994) 249.
[20] H. Thielking, D. Roessner, W.-M. Kulicke, Anal. Chem. 67 (1995) 3229.
[21] D.W. Shortt, D. Roessner, P.J. Wyatt, Am. Lab. 28 (17) (1996) 21.
[22] H. Thielking, W.-M. Kulicke, Anal. Chem. 68 (1996) 1169.
[23] K.D. Caldwell, in: H.G. Barth, J.W. Mays (Eds.), Modern Methods of Polymer Characterisation, Wiley, New York, 1991.
[24] J.C. Giddings, Science 260 (1993) 1456.
[25] P.S. Williams, J.C. Giddings, Anal. Chem. 66 (1994) 4215.
[26] R. Hecker, P.D. Fawell, A. Jefferson, J. Appl. Polym. Sci. 70 (1998) 2241.
[27] W.-M. Kulicke, R. Kniewske, J. Klein, Prog. Polym. Sci. 8 (1982) 373.
[28] R.-J. Müller, J. Klein, Makromol. Chem. 189 (1988) 2341.
[29] A. Peterlin, J. Polym. Sci., Part B: Polym. Phys. 4 (1966) 287.
[30] H.T. Sommer, C.F. Harrison, C.E. Montague, in: N.G. Stanley-Wood, R.W. Lines (Eds.), Particle Size Analysis, Royal Society of Chemistry, Cambridge, 1992.
[31] M. Chmelir, A. Künschner, E. Barthell, Angew. Makromol. Chem. 89 (1980) 145.
[32] D. Dupuis, F.Y. Lewandowski, P. Steiert, C. Wolff, J. Non-Newt. Fluid Mech. 54 (1994) 11.
[33] A.J. Muller, J.A. Odell, A. Keller, J. Non-Newt. Fluid Mech. 30 (1988) 99.
[34] P.J. Barham, Colloid Polym. Sci. 264 (1986) 917.
[35] J. François, D. Sarazin, T. Schwartz, G. Weill, Polymer 20 (1979) 969.
[36] R.C. Weast, M.J. Astle, CRC Handbook of Chemistry and Physics, CRC Press, Boca Raton, FL, 1982.
[37] E.S. Verstakov, Y.M. Kessler, Z.N. Kireeva, Z.A. Filimonova, Zh. Strukt. Khim. 22 (4) (1981) 180.
[38] E. Wieteska, in: G. Svehla (Ed.), Comprehensive Analytical Chemistry, Elsevier, Amsterdam, 1986, p. 391.
[39] K.D. Caldwell, S.L. Brimhall, Y. Gao, J.C. Giddings, J. Appl. Polym. Sci. 36 (1988) 703.
[40] W. Scholtan, Makromol. Chem. 14 (1954) 169.
[41] T. Schwartz, J. François, G. Weill, Polymer 21 (1980) 247.
[42] P.J. Wyatt, J. Colloid Interface Sci. 197 (1998) 9.
[43] Q. He, T.-S. Young, G.P. Willhite, D.W. Green, SPE Reservior Eng. 5 (1990) 333.